

ON THREE-PARAMETER FAMILIES OF FILIPPOV SYSTEMS – THE FOLD-SADDLE SINGULARITY.

CLAUDIO A. BUZZI¹, TIAGO DE CARVALHO² AND
MARCO A. TEIXEIRA³

ABSTRACT. This paper presents results concerning bifurcations of $2D$ piecewise-smooth vector fields. In particular, the generic unfoldings of codimension three fold-saddle singularities of Filippov systems, where a boundary-saddle and a fold coincide, are considered and the bifurcation diagrams exhibited.

1. INTRODUCTION

The general purpose of this paper is to study non-smooth vector fields (NSVF's for short), also called Filippov systems, Z represented by the following three-parameter family of differential equations in \mathbb{R}^2 :

$$(1) \quad \overline{Z}_{\lambda,\mu,\beta}^T = \begin{cases} X_\lambda = \begin{pmatrix} 1 \\ \alpha_1(\tau)(x-\lambda) + \alpha_2(\tau)(x-\lambda)^2 \end{pmatrix} & \text{if } y \geq 0, \\ Y_{\mu,\beta} = \begin{pmatrix} \frac{\mu}{2}x + \frac{(\mu-2)}{2}(y+\beta) \\ \frac{(\mu-2)}{2}x + \frac{\mu}{2}(y+\beta) \end{pmatrix} & \text{if } y \leq 0, \end{cases}$$

where $\tau = \{inv, vis\}$, $\alpha_1(inv) = -1$, $\alpha_1(vis) = 1$, $\alpha_2(inv) = 1$, $\alpha_2(vis) = 0$ and $(\lambda, \beta, \mu) \in (-1, 1) \times (-\sqrt{3}/2, \sqrt{3}/2) \times (-\varepsilon_0, 1)$ with $\varepsilon_0 > 0$ sufficiently small.

In Figure 1 (respectively, Figure 2) we consider $\lambda = \mu = \beta = 0$ and $\tau = inv$ (respectively, $\tau = vis$) in Equation (1).

Call $S_X = \{X^2 = 0\}$ and $S_Y = \{Y^2 = 0\}$ where $X_\lambda = X = (X^1, X^2)$ and $Y_{\mu,\beta} = Y = (Y^1, Y^2)$. Denote $\overline{Z}_{\lambda,\mu,\beta}^T = (X_\lambda, Y_{\mu,\beta}) = (X, Y)$. In short our goal is to study the local dynamics of $\overline{Z}_{\lambda,\mu,\beta}^T$ consisting of two smooth vector fields X_λ and $Y_{\mu,\beta}$ in \mathbb{R}^2 such that on one side of a smooth surface $\Sigma = \{y = 0\}$ we take $\overline{Z}_{\lambda,\mu,\beta}^T = X_\lambda$ and on the other side $\overline{Z}_{\lambda,\mu,\beta}^T = Y_{\mu,\beta}$. We mention two particular generic situations that occur in our system when $\beta \neq 0$. The first one is the *fold-fold singularity* (or two-fold singularity – see Definition 2), studied in some detail in [Guardia *et al.*(2011)] and [Kuznetsov *et al.*(2003)] (among others), in which the trajectories of both X and Y have a quadratic tangency to Σ at a point $p \in \Sigma$. The other

1991 *Mathematics Subject Classification.* Primary 34A36, 37G10, 37G05.

Key words and phrases. Fold-Saddle singularity, non-smooth vector fields, bifurcation, unfolding.

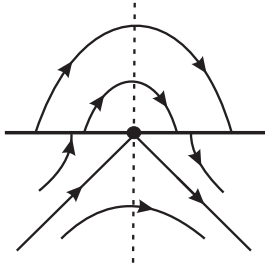


FIGURE 1. (Invisible)
Fold-Saddle Singularity.

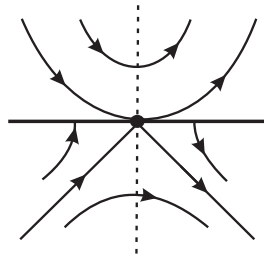


FIGURE 2. (Visible)
Fold-Saddle Singularity.

situation is the occurrence of branches of *canard cycles* (see Definition 5) which are typical minimal sets that appear in NSVF's.

It is worth saying that the set Ω^r of all NSVF's $Z = (X, Y)$ as below described (with some specified topology) is a differentiable manifold modeled in a Banach space (see Section 3 for details).

We now give a brief and rough overall description of the main features of this work:

- In Ω^r all NSVF's presenting a generic fold-saddle singularity form a codimension-three submanifold W_1 in such a way that any $Z \in W_1$ is locally equivalent (see Definition 8) to the above described $\overline{Z}_{\lambda, \mu, \beta}^r$ with $\lambda = \mu = \beta = 0$.
- The bifurcation diagram of $\overline{Z}_{\lambda, \mu, \beta}^r$ is exhibited for $\tau = inv$ and $\tau = vis$.

We emphasize that this paper is inserted in a larger 2D classification program where are included papers like [Teixeira(1977), Teixeira(1991), Kuznetsov *et al.*(2003), Guardia *et al.*(2011)]. One of the goals of this program is to classify (via topological equivalence) typical singularities of NSVF's. For this purpose it is necessary to present generic unfoldings and give non-degeneracy conditions on the system in order to characterize the codimension of the singularity. The bifurcation diagram of the codimension-three singularity presented here includes that one exhibited in [Guardia *et al.*(2011)]. The later claim is commented in the sequel. We finish this introduction presenting a physical model where a fold-saddle singularity can be found.

Example 1. *One of the reasons that second order linear equations with constant coefficients are worth studying is that they serve as mathematical models of some important physical processes. Two important areas of application are in the fields of mechanical and electrical oscillations. For example, the motion of a mass on a vibrating spring, the torsional oscillations of a shaft with a flywheel, the flow of electric current in a simple series circuit, and many other physical problems are all described by the solution of an equation of the form*

$$(2) \quad a\ddot{x} + b\dot{x} + cx = g(t, x).$$

Here we consider the external force g not depending on t but depending on x . For example consider

$$(3) \quad g(x) = Ax + 1 - \operatorname{sgn}(x) \text{ with } A > \frac{c}{a}.$$

Now if we call $\dot{x} = y$ then the equation (2) with g given by (3) became

$$(4) \quad \dot{x} = y, \quad \dot{y} = \left(A - \frac{c}{a}\right)x - \frac{b}{a}y, \quad \text{if } x > 0$$

and

$$(5) \quad \dot{x} = y, \quad \dot{y} = \left(A - \frac{c}{a}\right)x - \frac{b}{a}y + 2, \quad \text{if } x < 0.$$

System (4) has a saddle equilibrium at the origin because $A > \frac{c}{a}$. And system (5) has an invisible fold (see Definition 1) at the origin. If $g(x) = Ax - 1 + \operatorname{sgn}(x)$ with $A > \frac{c}{a}$ then it has a saddle equilibrium and a visible fold. \square

The paper is organized as follows: In Section 2 we present the main results of the paper. In Section 3 we give some basic concepts about NSVF's in order to setting the problem in Section 4. The remaining sections are dedicated to prove the main results of the paper.

2. STATEMENT OF THE MAIN RESULTS

In what follows consider

$$(6) \quad \mu_0(\beta) = 2 - (12\beta/(-3 + 6\beta + \sqrt{9 - 12\beta^2})).$$

Theorem 1. *Assume $\tau = \operatorname{inv}$ and $\mu = \mu_0(\beta)$ in Equation (1). Then its bifurcation diagram in the (λ, β) -plane contains 19 distinct phase portraits (see Figure 19).*

First of all observe that if $\beta > 0$ and $\lambda = -1/2 + \sqrt{9 - 12\beta^2}/6$ in Theorem 1, then the NSVF has a homoclinic loop surrounding a non hyperbolic singularity. So, it is easy to see that the cases covered by Theorem 1 do not represent the full unfolding of the (invisible) fold-saddle singularity and the next two theorems become necessary.

Theorem 2. *Assume $\tau = \operatorname{inv}$ and $\mu_0(\beta) < \mu < 1$ in Equation (1). Then its bifurcation diagram in the (λ, β) -plane contains 21 distinct phase portraits (see Figure 21).*

Theorem 3. *Assume $\tau = \operatorname{inv}$ and $-\varepsilon_0 < \mu < \mu_0(\beta)$ in Equation (1). Then its bifurcation diagram in the (λ, β) -plane contains 21 distinct phase portraits (see Figure 21).*

Remark 1. *The bifurcation diagrams exhibited in Theorems 2 and 3 present a homoclinic loop surrounding a hyperbolic singularity. Observe that, under the conditions of Theorem 2 (respectively, Theorem 3) this singularity is an attractor (respectively, repeller) as illustrated in Figure 3, cases (a) and (b). Moreover, when the parameter μ varies from $-\varepsilon_0$ to 1 there is an element $\mu_0(\beta) \in (-\varepsilon_0, 1)$, given by Equation (6), such that $\overline{Z}_{\lambda, \mu_0(\beta), \beta}^{inv}$ presents a like Hopf bifurcation phenomenon as illustrated in Figure 3. This phenomenon is fully treated in [Guardia et al.(2011)] and [Kuznetsov et al.(2003)] and it is not covered by Theorems 1, 2 and 3.*

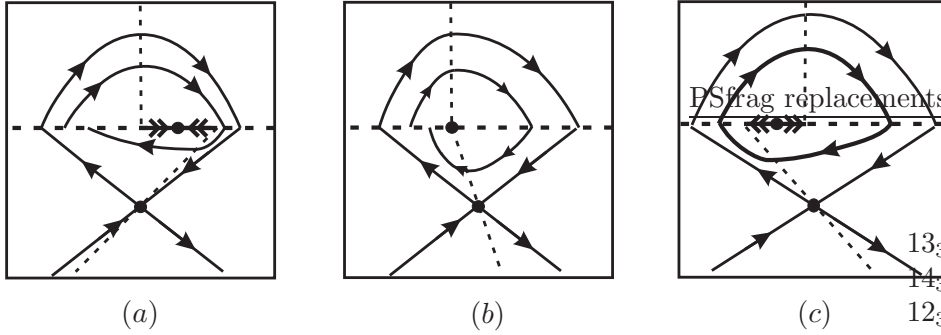


FIGURE 3. A like Hopf bifurcation. The singularities in (a) and (c) (that appear in Theorems 2 and 3 respectively) are called Σ -attractor and Σ -repeller throughout this paper (see Figure 5 cases (b) and (c)). In (b) we observe a non hyperbolic singularity present in Theorem 1.

Remark 2. *In Theorems 2 and 3 beyond the cases (a) and (c) in Figure 3, it also appears another relevant phenomenon that is the presence of a fold-fold singularity. Note that in Theorem 1 it occurs simultaneously the occurrence of a loop (a global phenomenon) and a fold-fold singularity (a local phenomenon).*

Theorem 4. *Assume $\tau = vis$ in Equation (11) or equivalently, take $\tau = vis$ and $\mu = 0$ in Equation (1). Then its bifurcation diagram in the (λ, β) -plane contains 13 distinct phase portraits (see Figure 27).*

The cases covered by Theorem 4 do not represent the full unfolding of the (visible) fold-saddle singularity. So, the next two theorems are necessary. Each one of them describes a distinct generic codimension two singularity.

Theorem 5. *Assume $\tau = vis$ and $0 < \mu < 1$ in Equation (1). Then its bifurcation diagram in the (λ, β) -plane contains 13 distinct phase portraits (see Figure 27).*

Theorem 6. *Assume $\tau = \text{vis}$ and $\varepsilon_0 < \mu < 0$ in Equation (1). Then its bifurcation diagram in the (λ, β) -plane contains 13 distinct phase portraits (see Figure 27).*

Remark 3. *In Theorems 5 and 6 one observes the birth of a singularity on Σ . This singularity behaves like a saddle (see Figure 5-(a)) and is known as Σ -saddle. This phenomenon does not occur under the conditions presented in Theorem 4.*

3. BASIC THEORY ABOUT NSVF

Let $K \subseteq \mathbb{R}^2$ be a compact set such that ∂K is a smooth curve. Consider $\Sigma \subseteq K$ given by $\Sigma = f^{-1}(0)$, where $f : K \rightarrow \mathbb{R}$ is a smooth function having $0 \in \mathbb{R}$ as a regular value (i.e. $\nabla f(p) \neq 0$, for any $p \in f^{-1}(0)$) such that $\partial K \cap \Sigma = \emptyset$ or $\partial K \pitchfork \Sigma$. Clearly the *switching manifold* Σ is the separating boundary of the regions $\Sigma_+ = \{q \in K \mid f(q) \geq 0\}$ and $\Sigma_- = \{q \in K \mid f(q) \leq 0\}$. We can assume that Σ is represented, locally around a point $q = (x, y)$, by the function $f(x, y) = y$.

Designate by χ^r the space of C^r -vector fields on K endowed with the C^r -topology with $r \geq 1$ large enough for our purposes. Call $\Omega^r = \Omega^r(K, f)$ the space of vector fields $Z : K \rightarrow \mathbb{R}^2$ such that

$$Z(x, y) = \begin{cases} X(x, y), & \text{for } (x, y) \in \Sigma_+, \\ Y(x, y), & \text{for } (x, y) \in \Sigma_-, \end{cases}$$

where $X = (X^1, X^2)$ and $Y = (Y^1, Y^2)$ are in χ^r . We write $Z = (X, Y)$, which we will accept to be multivalued in points of Σ . The trajectories of Z are solutions of $\dot{q} = Z(q)$, which has, in general, discontinuous right-hand side. The basic results of differential equations, in this context, were stated by Filippov in [Filippov(1988)]. Related theories can be found in [Kozlova(1984), Teixeira(1991)] among others.

3.1. Orbits, trajectories and singularities of NSVF's. In what follows we will use the notation

$$X.f(p) = \langle \nabla f(p), X(p) \rangle \quad \text{and} \quad X^i.f(p) = \langle \nabla(X^{i-1}.f)(p), X(p) \rangle, \quad i \geq 2$$

where $\langle \cdot, \cdot \rangle$ is the usual inner product in \mathbb{R}^2 .

Following the Filippov rule, we distinguish the following regions on the discontinuity set Σ :

- **Crossing region:** $\Sigma_c = \{p \in \Sigma \mid (X.f(p))(Y.f(p)) > 0\}$.
- **Escaping region:** $\Sigma_e = \{p \in \Sigma \mid X.f(p) > 0 \text{ and } Y.f(p) < 0\}$.
- **Sliding region:** $\Sigma_s = \{p \in \Sigma \mid X.f(p) < 0 \text{ and } Y.f(p) > 0\}$.

Consider $Z = (X, Y) \in \Omega^r$ and $p \in \Sigma_e \cup \Sigma_s$. The *sliding vector field* Z^Σ associated to Z at p is the convex combination of $X(p)$ and $Y(p)$ tangent to Σ at p (see Figure 4).

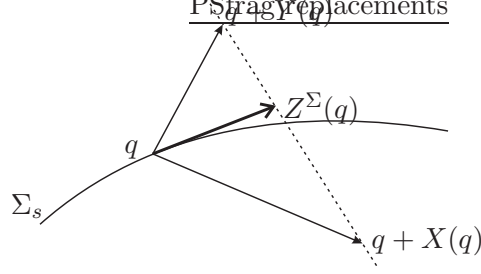


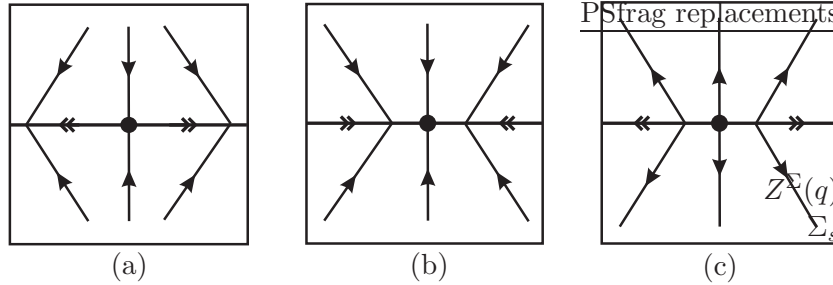
FIGURE 4. Filippov's convention.

We say that $q \in \Sigma$ is a Σ -regular point if

- $(X.f(q))(Y.f(q)) > 0$ or
- $(X.f(q))(Y.f(q)) < 0$ and $Z^\Sigma(q) \neq 0$ (that is $q \in \Sigma_e \cup \Sigma_s$ and it is not an equilibrium point of Z^Σ).

The points of Σ which are not Σ -regular are called Σ -singular. We distinguish two subsets in the set of Σ -singular points: Σ^t and Σ^p . Any $q \in \Sigma^p$ is called a *pseudo equilibrium* of Z and it is characterized by $Z^\Sigma(q) = 0$. Any $q \in \Sigma^t$ is called a *tangential singularity* and is characterized by $Z^\Sigma(q) \neq 0$ and $(X.f(q))(Y.f(q)) = 0$.

A pseudo equilibrium $q \in \Sigma^p$ is a Σ -saddle provided that one of the following condition is satisfied: (i) $q \in \Sigma_e$ and q is an attractor for Z^Σ or (ii) $q \in \Sigma_s$ and q is a repeller for Z^Σ . A pseudo equilibrium $q \in \Sigma^p$ is a Σ -repeller (resp. Σ -attractor) provided $q \in \Sigma_e$ (resp. $q \in \Sigma_s$) and q is a repeller (resp. attractor) equilibrium point for Z^Σ (see Figure 5).

FIGURE 5. Pseudo equilibria: (a) Σ -saddle, (b) Σ -attractor and (c) Σ -repeller.

Definition 1. We say that $p_0 \in \Sigma^t$ is a Σ -fold point of $X \in \chi^r$ if $X.f(p_0) = 0$ but $X^2.f(p_0) \neq 0$. Moreover, $p_0 \in \Sigma$ is a visible (respectively invisible) Σ -fold point of X if $X.f(p_0) = 0$ and $X^2.f(p_0) > 0$ (respectively $X^2.f(p_0) < 0$).

Definition 2. Let $Z = (X, Y) \in \Omega^r$. We say that $p \in \Sigma^t$ is a **fold-fold singularity** of Z if p is a Σ -fold point for both X and Y .

Definition 3. Let $Z = (X, Y) \in \Omega^r$. We say that $q \in \Sigma$ is a **fold-saddle singularity** of Z if q is a Σ -fold point of X and a saddle equilibrium of Y (in this case q is called a *boundary-saddle* of Y).

The following construction is presented in [Teixeira(2008)]. Let $Z = (X, Y) \in \Omega^r$ such that T is an invisible Σ -fold point of X . From Implicit Function Theorem, for each $p \in \Sigma$ in a neighborhood \mathcal{V}_T of T we derive that there exists a unique $t(p)$ such that the orbit-solution $t \mapsto \varphi_X(t, p)$ of X through p meets Σ at a point $\tilde{p} = \varphi_X(t(p), p)$. Define the map $\gamma_X : \mathcal{V}_T \cap \Sigma \rightarrow \mathcal{V}_T \cap \Sigma$ by $\gamma_X(p) = \tilde{p}$. This map is a C^r -diffeomorphism and satisfies: $\gamma_X^2 = Id$. Analogously, when \tilde{T} is an invisible Σ -fold point of Y we define the map $\gamma_Y : \mathcal{V}_{\tilde{T}} \cap \Sigma \rightarrow \mathcal{V}_{\tilde{T}} \cap \Sigma$ associated to Y which satisfies $\gamma_Y^2 = Id$. We define now the first return map associated to $Z = (X, Y)$:

Definition 4. The **first return map** $\varphi_Z : \mathcal{T} \rightarrow \mathcal{T}$ is defined by the composition $\varphi_Z = \gamma_Y \circ \gamma_X$ when both γ_X and γ_Y are well defined in $\mathcal{T} \subset \Sigma$.

Remark 4. φ_Z is an area-preserving map.

Definition 5. A curve Γ is a **canard cycle** of $Z = (X, Y) \in \Omega^r$ if it is closed and composed by orbit-arcs of at least two of the vector fields $X|_{\Sigma_+}$, $Y|_{\Sigma_-}$ and Z^Σ . We say that Γ is **hyperbolic** if $\varphi'_Z(p) \neq 1$, where φ_Z is the first return map defined on a segment T with $p \in T \cap \gamma$.

Definition 6. Consider $Z \in \Omega^r$. A closed path Δ is a **Σ -graph** if it is a union of equilibria, pseudo equilibria, tangential singularities of Z and orbit-arcs of Z joining these points in such a way that $\Delta \cap \Sigma \neq \emptyset$.

Definition 7. Consider $Z \in \Omega^r$. A point $q \in \Sigma$ is a **Σ -center** if there is a neighborhood U of q filled up with a one-parameter family γ_U of canard cycles of Z in such a way that $\gamma_U \cap \Sigma \subset \Sigma_c$ (see Figure 7).

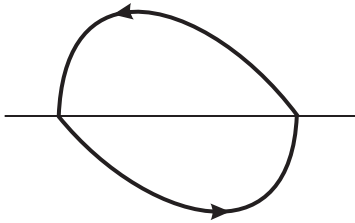


FIGURE
6. Canard
cycle.

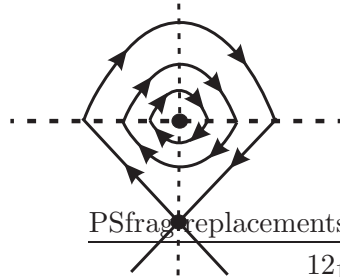


FIGURE 7. Σ -graph
surrounding a Σ -center.

3.2. Structural Stability on Ω^r . Bifurcation theory describes how continuous variations of parameter values in a dynamical system can, through topological changes, cause the phase portrait to change suddenly. In this paper we focus on certain structurally unstable NSVF's within a generic context. In [Andronov & Pontryagin(1937)] the concept of k^{th} -order structural stability is presented; in a local approach such setting gives rise to the notion of a codimension k singularity. Now we present the concept of equivalence which will guide us for all the paper.

Definition 8. *Two NSVF's $Z, \tilde{Z} \in \Omega^r(K, f)$ defined in open sets $U, \tilde{U} \subset K$ with switching manifolds $\Sigma \subset U$ and $\tilde{\Sigma} \subset \tilde{U}$ respectively are Σ -**equivalent** if there exists an orientation preserving homeomorphism $h : U \rightarrow \tilde{U}$ which sends Σ to $\tilde{\Sigma}$ and sends orbits of Z (respectively Z^Σ) to orbits of \tilde{Z} (respectively $\tilde{Z}^{\tilde{\Sigma}}$). From this definition the concept of **local structural stability** in Ω^r is naturally obtained.*

As we said in Section 1 our paper is a generalization of some papers that unfold typical singularities of NSVF's. Below we present the program used in the literature and in our paper to exhibit the diagram bifurcation of a singularity of NSVF's.

Let $Z \in \Omega^r$ and $p \in \Sigma$. Following the approach in [Sotomayor(1974)] (and also exposed in [Guardia *et al.*(2011)], Subsection 3.1, pg 1982), we get that:

- By Theorem 3.5 of [Guardia *et al.*(2011)] we already know the characterization of the set $\Phi_0^p = \{Z \in \Omega^r \mid Z \text{ is locally structurally stable at } p\}$. In fact, Φ_0^p is open and dense in Ω^r . So, Φ_0^p is the codimension zero local bifurcation set.
- Let $\Omega_1 = \Omega^r \setminus \Phi_0^p$ and $\Phi_1^p = \{Z \in \Omega_1 \mid Z \text{ is locally structurally stable at } p \text{ relative to } \Omega_1\}$. The set Φ_1^p is the codimension 1 local bifurcation set in Ω^r . The characterization Φ_1^p was given in [Kuznetsov *et al.*(2003)].
In addition, if $Z_0 \in \Phi_1^p$, it is also known (see [Teixeira(1979)]) that there exists a neighborhood \mathcal{U} of Z_0 in Ω^r such that:
 - There exists a C^r -function $L : \mathcal{U} \rightarrow \mathbb{R}$, satisfying $L(Z_0) = 0$ and DL_{Z_0} , the differential of L at Z_0 , is surjective. Moreover, $L^{-1}(0) = \Phi_1^p \cap \mathcal{U}$.
 - Consider now all the embeddings $\Theta : (-\varepsilon, \varepsilon) \times \mathcal{U} \rightarrow \mathcal{U}$ transversal to Φ_1^p at some $Z \in \Phi_1^p$ and such that $\Theta(0, Z_0) = Z$. We refer to such Θ as an *unfolding* of Z_0 .
- We consider now the set $\Omega_2 = \Omega_1 \setminus \Phi_1^p$ and similar objects Φ_2^p (the set of codimension 2 singularities) and families of objects $L : \mathcal{U} \rightarrow \mathbb{R}^2$, with surjective derivative at Z_0 and embeddings $\Theta : (-\varepsilon, \varepsilon) \times (-\zeta, \zeta) \times \mathcal{U} \rightarrow \mathcal{U}$.
- In this way we can get sequences Ω_k and Φ_k^p in Ω^r , that establish a program to characterize all codimension k singularities.

Definition 9. Let $\mathcal{V}(0, \mathbb{R}^k)$ and $\mathcal{S}(0, \mathbb{R}^l)$ be neighborhoods of 0 in \mathbb{R}^k and \mathbb{R}^l respectively and let \mathcal{U} be a neighborhood of Z_0 in Ω^r . We say that two **unfoldings** $\Theta : \mathcal{V}(0, \mathbb{R}^k) \times \mathcal{U} \rightarrow \mathcal{U}$ and $\Xi : \mathcal{S}(0, \mathbb{R}^l) \times \mathcal{U} \rightarrow \mathcal{U}$ are **equivalent** if there is a homomorphism $A : \mathcal{V}(0, \mathbb{R}^k) \rightarrow \mathcal{S}(0, \mathbb{R}^l)$ such that $A(\lambda) = \mu$ and for each $Z \in \mathcal{U}$ the vector fields $\Theta(\lambda, Z)$ and $\Xi(A(\lambda), Z)$ are Σ -equivalent according to Definition 8. Moreover, we say that an unfolding $\Theta(\lambda_0, \cdot)$ is a **generic unfolding** if there is a neighborhood $\mathcal{W}(\Theta(\lambda_0, \cdot))$ of $\Theta(\lambda_0, \cdot)$ such that any unfolding $\Theta(\lambda, \cdot) \in \mathcal{W}(\Theta(\lambda_0, \cdot))$ is equivalent to $\Theta(\lambda_0, \cdot)$.

Remark 5. In Definition 9 it is important to say that the homomorphism A does not vary, necessarily, continuously with respect to the parameter $\lambda \in \mathcal{V}(0, \mathbb{R}^k)$.

3.3. The Direction Function H . Here we introduce a function that will be very useful in the sequel.

In $(A, B) \subset \Sigma_e \cup \Sigma_s$, consider the point $C = (C_1, C_2)$, the vectors $X(C) = (D_1, D_2)$ and $Y(C) = (E_1, E_2)$ (as illustrated in Figure 8). The straight segment passing through $C + X(C)$ and $C + Y(C)$ meets Σ in a point $p(C)$. We define the C^r -map

$$p : \begin{array}{ccc} (A, B) & \longrightarrow & \Sigma \\ z & \longmapsto & p(z). \end{array}$$

Since Σ is the x -axis, we have that $C = (C_1, 0)$ and $p(C) \in \mathbb{R} \times \{0\}$ can be identified with points in \mathbb{R} . According with this identification, the *direction function* on Σ is defined by

$$H : \begin{array}{ccc} (A, B) & \longrightarrow & \mathbb{R} \\ z & \longmapsto & p(z) - z. \end{array}$$

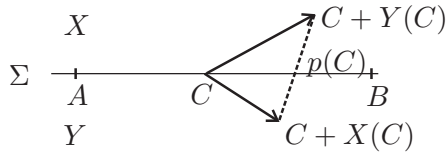


FIGURE 8. Direction function.

We obtain that H is a C^r -map and

- if $H(C) < 0$ then the orientation of Z^Σ in a small neighborhood of C is from B to A ;
- if $H(C) = 0$ then $C \in \Sigma^p$;
- if $H(C) > 0$ then the orientation of Z^Σ in a small neighborhood of C is from A to B .

Simple calculations show that $p(C_1) = \frac{E_2(D_1+C_1)-D_2(E_1+C_1)}{E_2-D_2}$ and consequently,

$$(7) \quad H(C_1) = \frac{E_2D_1 - D_2E_1}{E_2 - D_2}.$$

Remark 6. *If $X.f(p) = 0$ and $Y.f(p) \neq 0$ then, in a neighborhood V_p of p in Σ , the direction function H has the same sign of D_1 , where $X(p) = (D_1, D_2)$. In fact, $X.f(p) = 0$ and $Y.f(p) \neq 0$ are equivalent to $D_2 = 0$ and $E_2 \neq 0$ in (7). So, $\lim_{(D_2, E_2) \rightarrow (0, k_0)} H(p_1) = D_1$, where $k_0 \neq 0$ and $p = (p_1, p_2)$.*

4. SETTING THE PROBLEM

Let $\Gamma_+ = \{X|_{\Sigma_+} \text{ with } X \in \chi^r\}$ (respectively, $\Gamma_- = \{X|_{\Sigma_-} \text{ with } X \in \chi^r\}$). This means that Γ_+ (respectively, Γ_-) is identified with χ^r .

Let $\Gamma_{\Sigma_+}^F \subset \Gamma_+$ be the set of all elements $X \in \Gamma_+$ having a Σ -fold point. $\Gamma_{\Sigma_+}^F$ is an open set in Γ_+ (see [Teixeira(1977)]). We may consider $f(x, y) = y$ and the following generic normal forms $X_0(x, y) = (\alpha_1, \beta_1 x)$ with $\alpha_1 = \pm 1$ and $\beta_1 = \pm 1$ (see [Vishik(1972)], Theorem 2).

Let $\Gamma_{\Sigma_-}^S \subset \Gamma_-$ be the set of all elements $Y \in \Gamma_-$ presenting a hyperbolic saddle equilibrium S_{Y_0} on Σ (called *boundary saddle* in the literature – as a reference, in [Roy & Roy(2008)], are exhibited some border collisions in three-dimension NSVF's) and such that the eigenspaces of $DY_0(S_{Y_0})$ are transverse to Σ at S_{Y_0} . $\Gamma_{\Sigma_-}^S$ is a codimension one submanifold of Γ_- . Note that, $\Gamma_{\Sigma_-}^S$ has a C^r -structure (for more details about this construction see [Dumortier (1978)]). In fact, since Y_0 has a hyperbolic boundary saddle S_{Y_0} and the eigenspaces of $DY_0(S_{Y_0})$ are transverse to Σ at S_{Y_0} , then there exists a neighborhood $\mathcal{V}(Y_0)$ of Y_0 in χ^r such that all $Y \in \mathcal{V}(Y_0)$ have a hyperbolic boundary saddle $S_Y = (x^*, y^*)$ with the same properties of the eigenspaces. Moreover, the correspondence $L : \mathcal{V}(Y_0) \rightarrow \mathbb{R}^2$, given by $L(Y) = S_Y$, is C^r at Y_0 . Define $\Pi : \mathcal{V}(Y_0) \rightarrow \mathbb{R}$, given by $\Pi(Y) = (f \circ L)(Y)$. We say that two vector fields $Y, \tilde{Y} \in \Gamma_{\Sigma_-}^S$ defined in open sets U and \tilde{U} , respectively, are C^0 -orbitally equivalent if there exists an orientation preserving homeomorphism $h : U \rightarrow \tilde{U}$ that sends orbits of Y to orbits of \tilde{Y} . From [Teixeira(1977)] we know that any $Y \in \Gamma_{\Sigma_-}^S$ is generically C^0 -orbitally equivalent to its linear part by a Σ -preserving homeomorphism. And the linear saddle with eigenspaces transverse to the x -axis has the generic normal forms $Y_0(x, y) = (\alpha_2 y, \alpha_2 x)$ with $\alpha_2 = \pm 1$. So it is easy to see that the generic unfolding of the singularity is given by $Y_\beta = (\alpha_2(y + \beta), \alpha_2 x)$ where $\beta \in \mathbb{R}$.

Moreover:

- There exists a C^r -function $\Pi : \mathcal{V}(Y_0) \rightarrow \mathbb{R}$, such that $D\Pi|_{Y_0}$ is surjective.
- The correspondence $Y \mapsto S_Y$ is C^r , where S_Y is a saddle point of Y .

- If $\Pi(Y) < 0$ then $S_Y \in \Sigma_-$.
- If $\Pi(Y) = 0$ then $S_Y \in \Sigma$.
- If $\Pi(Y) > 0$ then $S_Y \in \Sigma_+$.

In this paper we are concerned with the bifurcation diagram of systems $Z_0 = (X_0, Y_0)$ in Ω^r such that $X_0 \in \Gamma_{\Sigma_+}^F$, $Y_0 \in \Gamma_{\Sigma_-}^S$ and $p_0 = S_{Y_0} \in \Sigma$. The fold-saddle singularity $p_0 = S_{Y_0}$ is illustrated in Figures 1 and 2 – the dotted lines in these and later figures represent the points where $X.f = 0$ and $Y.f = 0$.

Let $p = (0, 0)$ be a fold-saddle singularity of $Z = (X, Y)$. We denote the set of all NSVF $Z = (X, Y)$ such that $X \in \Gamma_{\Sigma_+}^F$ and $Y \in \Gamma_{\Sigma_-}^S$ by Γ^{F-S} . We endow $\chi^r \times \chi^r$ (consequently Ω^r and Γ^{F-S}) with the product topology. Let $Z_0 = (X_0, Y_0) \in \Gamma^{F-S}$. Observe that 0 is the unique singularity of X_0 around a neighborhood W_0 of the origin in \mathbb{R}^2 . So, there exists a neighborhood U_0 of Z_0 in Ω^r such that for any $Z = (X, Y) \in U_0$ we may find a Σ -fold point $p_Z = (k_Z, 0) \in W_0$ such that it is the unique singularity of X in W_0 . Moreover the correspondence $Z \mapsto p_Z$ is C^r .

In the same way, for any $Z = (X, Y) \in U_0$ we find a C^r -correspondence $B : U_0 \rightarrow \mathbb{R}^2$ where $B(Z) = s_Z = (a_Z, b_Z)$ is the (unique) equilibrium (saddle) of Y in U_0 . We are assuming that the eigenspaces of $DY_{s_Z}(q_Z)$ are transverse to Σ at s_Z . We have to distinguish the cases: (i) $b_Z < 0$, (ii) $b_Z = 0$ and (iii) $b_Z > 0$. Observe that when $b_Z < 0$ (resp. $b_Z > 0$) there is associated to Z an invisible (resp. visible) Σ -fold point of Y given by $q_Y = (c_Z, 0) \in W_0$. Moreover $\lim_{b_Z \rightarrow 0} c_Z = a_Z$.

Define $F(Z) = (k_Z - a_Z, b_Z)$. Knowing that s_Z is a hyperbolic equilibrium point of Z and 0 is a regular value of F , it is not hard to prove (see [Teixeira(1979)]) that:

- The derivative $DF : U_0 \rightarrow \mathbb{R}^2$ is surjective and
- $F^{-1}(0) = \Omega_2$ is a codimension two submanifold of Ω^r .

Therefore this fold-saddle singularity occurs generically in two-parameter families of vector fields in Ω^r .

4.1. Normal Form. We start this section with the following model:

$$(8) \quad Z^\tau = \begin{cases} X^\tau = \begin{pmatrix} \rho_1 \\ \alpha_1(\tau)x \end{pmatrix} & \text{if } y \geq 0, \\ Y = \begin{pmatrix} k_1 y \\ k_1 x \end{pmatrix} & \text{if } y \leq 0, \end{cases}$$

where $\tau = \{inv, vis\}$, $\alpha_1(inv) = -1$, $\alpha_1(vis) = 1$, $\rho_1 = \pm 1$ and $k_1 = \pm 1$.

The next lemma provides explicitly the equivalence between $Z \in \Omega_2$ and the model (8). We present an outline of proof of the previous lemma in Section 5.

Lemma 1. *If $Z \in \Omega_2$ then Z is Σ -equivalent to Z^τ given by (8).*

Note that there exists a NSVF $\tilde{Z} \in \Omega^r$ nearby Z^{inv} , given by (8), such that \tilde{Z} presents a Σ -center (see Figure 7). In fact, this suggests that the unfolding of (8) has infinite codimension. At this point it seems natural to propose the following conjecture.

Conjecture: *For any neighborhood $\mathcal{W} \subset \Omega^r$ of Z^{inv} (given by (8)), and for any integer $k > 0$ there exists $\tilde{Z} \in \mathcal{W}$ such that the codimension of \tilde{Z} is k .*

So, based on this conjecture, we have to sharpen our normal normal. In fact, in order to get low codimension bifurcation we have to impose some generic assumptions.

Without loss of generality, throughout the rest of this paper we consider $\rho_1 = 1$ and $k_1 = -1$ at the model (8). The other choices of the parameters are treated analogously. When $\tau = inv$ we add the extra generic assumption $X_0^3 \cdot f(p) \neq 0$ on the Σ -fold point p of $Z_0 = (X_0, Y_0) \in \Gamma^{F-S}$. By means of Theorem 2 in [Vishik(1972)], we may conclude that around the invisible Σ -fold point the vector field X_0 can be expressed as $X_0 = (1, -x + a_1 x^2)$ and $f(x, y) = y$, where $a_1 \neq 0$. We say that X_0 is *contractive* (respectively, *expansive*) at p if $a_1 < 0$ (respectively $a_1 > 0$).

According to the previous discussion, we will consider $Z_0^{inv}, Z_0^{vis} \in \Omega^r$ written in the following forms:

$$(9) \quad Z_0^{inv} = \begin{cases} X_0^{inv} = \begin{pmatrix} 1 \\ -x + x^2 \end{pmatrix} & \text{if } y \geq 0, \\ Y_0 = \begin{pmatrix} -y \\ -x \end{pmatrix} & \text{if } y \leq 0, \text{ and} \end{cases}$$

$$(10) \quad Z_0^{vis} = \begin{cases} X_0^{vis} = \begin{pmatrix} 1 \\ x \end{pmatrix} & \text{if } y \geq 0, \\ Y_0 = \begin{pmatrix} -y \\ -x \end{pmatrix} & \text{if } y \leq 0. \end{cases}$$

Note that X_0^{inv} presents an invisible expansive Σ -fold point in its phase portrait and X_0^{vis} presents a visible one.

4.2. Unfoldings. The main question of this paper is to exhibit the bifurcation diagram of Z_0^τ with either $\tau = inv$ or $\tau = vis$. For this reason we consider unfoldings of the normal forms (9) and (10). We obtain that:

I- There is an imbedding $F_0^\tau : \mathbb{R}^2, 0 \rightarrow \chi^r, Z_0^\tau$ such that $F_0^\tau(\lambda, \beta) = Z_{\lambda, \beta}^\tau$ is expressed by:

$$(11) \quad Z_{\lambda, \beta}^\tau = \begin{cases} X_\lambda^\tau = \begin{pmatrix} 1 \\ \alpha_1(\tau)(x - \lambda) + \alpha_2(\tau)(x - \lambda)^2 \end{pmatrix} & \text{if } y \geq 0, \\ Y_\beta = \begin{pmatrix} -(y + \beta) \\ -x \end{pmatrix} & \text{if } y \leq 0, \end{cases}$$

where $\tau = \{inv, vis\}$, $(\lambda, \beta) \in (-1, 1) \times (-\sqrt{3}/2, \sqrt{3}/2)$, $\alpha_1(inv) = -1$, $\alpha_1(vis) = 1$, $\alpha_2(inv) = 1$ and $\alpha_2(vis) = 0$. Moreover, the two-parameter family given by (11) is transversal to Ω_2 . We stress that in [Guardia *et al.*(2011)] the unfolding of the case $\tau = inv$ is done. Nevertheless we observe that there are some typical topological types nearby Z_0^τ that do not appear in the bifurcation diagram of $Z_{\lambda, \beta}^\tau$. For example, when $\tau = inv$ the configurations in Figure 9 cases (a) and (b) are excluded and when $\tau = vis$ the configuration in Figure 9–(c) also is excluded.

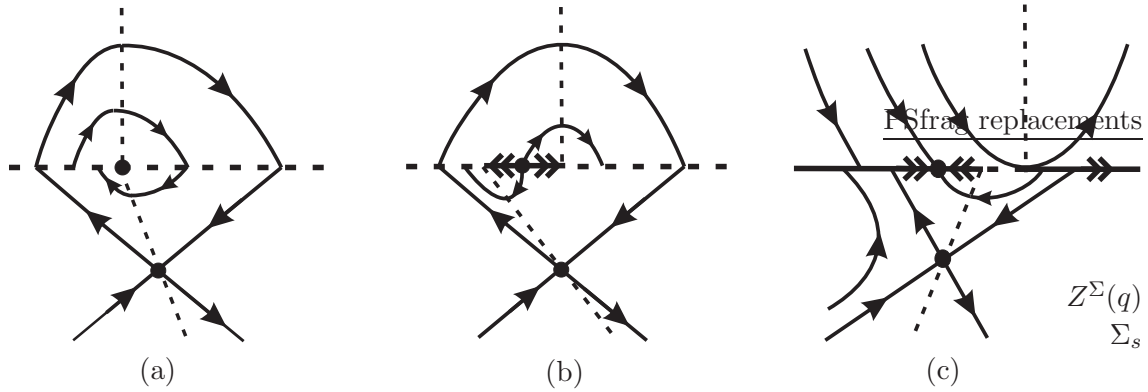


FIGURE 9. Cases do not covered in [Guardia *et al.*(2011)]. In (a) and (b) (respectively, in (c)) the fold singularity is invisible (respectively, visible).

II- In order to consider a more general situation which includes the above mentioned cases we add an auxiliary parameter μ . As a result the model in Equation 1 is obtained.

We stress that the configuration illustrated in Figure 9–(a) plays a very important role in our analysis. In this *resonant* configuration we note, simultaneously, a fold-fold singularity (which is a local phenomenon) and a Σ –graph (loop) passing through the saddle equilibrium (which is a global phenomenon). Only the bifurcation of these two unstable configurations already represents a relevant development (the fold-fold singularity was studied recently in [Guardia *et al.*(2011)] and the *non-smooth loop bifurcation*, as far as we know, was not studied until the present work). In fact, this configuration is reached in (1), taking $\mu = \mu_0(\beta)$.

In what follows, in order to simplify the calculations, we take $\mu = \alpha + 1$ in (1) and obtain the following expression:

$$(12) \quad Z_{\lambda,\alpha,\beta}^{\tau} = \begin{cases} X_{\lambda} = \begin{pmatrix} 1 \\ \alpha_1(\tau)(x - \lambda) + \alpha_2(\tau)(x - \lambda)^2 \end{pmatrix} & \text{if } y \geq 0, \\ Y_{\alpha,\beta} = \begin{pmatrix} \frac{(1+\alpha)}{2}x + \frac{(-1+\alpha)}{2}(y + \beta) \\ \frac{(-1+\alpha)}{2}x + \frac{(1+\alpha)}{2}(y + \beta) \end{pmatrix} & \text{if } y \leq 0, \end{cases}$$

where $\tau = \{inv, vis\}$, $\alpha_1(inv) = -1$, $\alpha_1(vis) = 1$, $\alpha_2(inv) = 1$, $\alpha_2(vis) = 0$ and $(\lambda, \beta, \alpha) \in (-1, 1) \times (-\sqrt{3}/2, \sqrt{3}/2) \times (-1 - \varepsilon_0, 1)$ with $\varepsilon_0 > 0$ sufficiently small. Since $\mu_0(\beta)$ is given by (6), we obtain that

$$(13) \quad \alpha_0(\beta) = 1 - (12\beta / (-3 + 6\beta + \sqrt{9 - 12\beta^2})).$$

When it does not produce confusion, in order to simplify the notation we use $Z = (X, Y)$ or $Z_{\lambda,\alpha,\beta} = (X, Y)$ instead $Z_{\lambda,\alpha,\beta}^{\tau} = (X_{\lambda}, Y_{\alpha,\beta})$.

4.2.1. *Geometrical Analysis of the Normal Form (12)*. Given $Z = (X, Y)$, we describe some properties of both $X = X_{\lambda}$ and $Y = Y_{\alpha,\beta}$.

The real number λ measures how the Σ -fold point $d = (d_1, d_2) = (\lambda, 0)$ of X is translated away from the origin. More specifically, if $\lambda < 0$ then d is translated to the left hand side and if $\lambda > 0$ then d is translated to the right hand side.

Some calculations show that the curve $Y.f = 0$ is given by $y = \frac{(1-\alpha)}{(1+\alpha)}x - \beta$. So the points of this curve are equidistant from the separatrices when $\alpha = -1$. It becomes closer to the stable separatrix of the saddle equilibrium $S = S_{\alpha,\beta} = (s_1, s_2)$ when $\alpha \in (-1, 0)$. It becomes closer to the unstable separatrix of S when $\alpha \in (-1 + \varepsilon_0, -1)$. Moreover, the smooth vector field Y has distinct types of contact with Σ according to the particular deformation considered. In this way, we have to consider the following behaviors:

- \mathbf{Y}^- : In this case $\beta < 0$. So S is translated to the y -direction with $y > 0$ (and S is not visible for Z). It has a visible Σ -fold point $e = e_{\alpha,\beta} = (e_1, e_2) = \left(\frac{(1+\alpha)}{(1-\alpha)}\beta, 0\right) = (e_1, 0)$ (see Figure 10).
- \mathbf{Y}^0 : In this case $\beta = 0$. So S is not translated (see Figure 1).
- \mathbf{Y}^+ : In this case $\beta > 0$. So S is translated to the y -direction with $y < 0$. It has an invisible Σ -fold point $i = i_{\alpha,\beta} = (i_1, i_2) = \left(\frac{(1+\alpha)}{(1-\alpha)}\beta, 0\right)$. Moreover, we distinguish two points: $h = h_{\beta} = (h_1, h_2) = (-\beta, 0)$ which is the intersection between the unstable separatrix with Σ and $j = j_{\beta} = (j_1, j_2) = (\beta, 0)$ which is the intersection between the stable separatrix with Σ (see Figure 11).

In Figure 11 we distinguish the arcs of trajectory σ_1 joining S to h and σ_2 joining j to S .

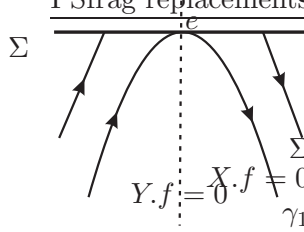


FIGURE 10. Case Y^- : perturbation of a boundary saddle generating a visible fold.

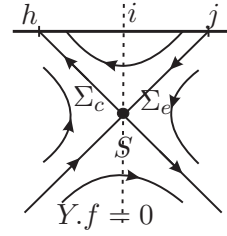
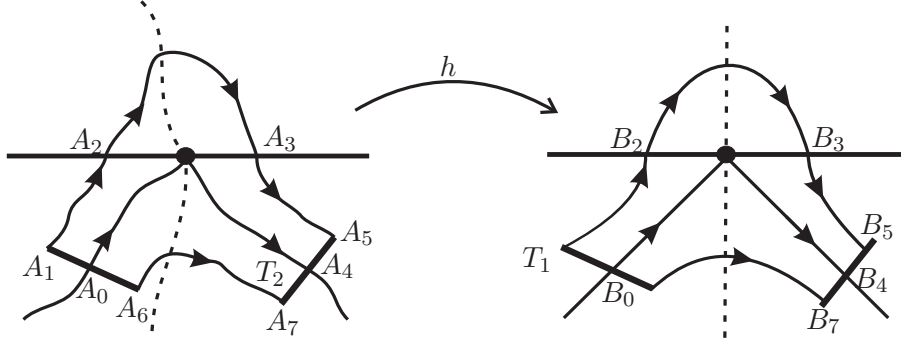


FIGURE 11. Case Y^+ : perturbation of a boundary saddle generating an invisible fold.

5. PROOF OF LEMMA 1

Now, we show how we can construct the homeomorphism in Lemma 1.

Outline of Proof of Lemma 1. Here we construct a Σ -preserving homeomorphism h that sends orbits of $Z = (X, Y) \in \Omega_2$, defined in a sufficiently small neighborhood \mathcal{U}_0 of the fold-cusp singularity of Z , to orbits of $\tilde{Z} = (\tilde{X}, \tilde{Y})$, defined in a sufficiently small neighborhood $\tilde{\mathcal{U}}_0$ of the fold-cusp singularity of \tilde{Z} , where $\tilde{Z} = Z^{inv}$ is given by (8) with $\rho_1 = 1$ and $k_1 = -1$ (the other cases are treated analogously). Consider A_0 an arbitrary point of the stable separatrix of the saddle point S of Y (see Figure 12). Let T_1 be a transversal section of Y at A_0 . The section T_1 also is transversal to \tilde{Y} and it crosses the stable separatrix of the saddle point \tilde{S} of \tilde{Y} at B_0 . Let $A_1 \in T_1$ be a point on the left of A_0 . The trajectory of Y passing through A_1 crosses Σ at A_2 . In the same way, the trajectory of \tilde{Y} passing through B_1 crosses Σ at B_2 . The trajectory of X that passes through A_2 crosses Σ in a point A_3 . The trajectory of \tilde{X} that passes through B_2 crosses Σ in B_3 . Consider A_4 an arbitrary point of the unstable separatrix of S . Let T_2 be a transversal section of Y passing through A_4 . The section T_2 also is transversal to \tilde{Y} and it crosses the unstable separatrix of \tilde{S} at the point B_4 . The trajectory of Y passing through A_3 crosses T_2 in a point A_5 . In the same way, the trajectory of \tilde{Y} passing through B_3 crosses T_2 at B_5 . Let $A_6 \in T_1$ be a point at the right of A_0 . The trajectory of Y passing through A_6 crosses T_2 at A_7 . The trajectory of \tilde{Y} passing through A_6 crosses T_2 at B_7 . The homeomorphism h sends T_1 to T_1 , the arc of trajectory $\gamma_1 = \widehat{A_1 A_5}$ to the arc of trajectory $\tilde{\gamma}_1 = \widehat{A_1 B_5}$ and the arc of trajectory $\gamma_2 = \widehat{A_6 A_7}$ to the arc of trajectory $\tilde{\gamma}_2 = \widehat{A_6 B_7}$. Now we can extend continuously h to the interior of the region bounded by $T_1 \cup \gamma_1 \cup T_2 \cup \gamma_2$. In this way, there exists a Σ -preserving homeomorphism h that sends orbits of Z to orbits of \tilde{Z} .

FIGURE 12. Construction of a C^0 -equivalence: Case $\tau = inv$.

When $\tilde{Z} = Z^{vis}$ is given by (8), the first coordinate of \tilde{X} is equal to 1 and $k_1 = -1$. We build the same above construction until the appearance of A_2 and B_2 . Now, consider C_4 an arbitrary point of the stable separatrix of the Σ -fold point F of X (see Figure 13). Let T_3 be a transversal section to X at C_4 . The section T_3 is also transversal to \tilde{X} and it crosses the stable separatrix of the Σ -fold point \tilde{F} of \tilde{X} at the point D_4 . The trajectory of X passing through A_2 crosses T_3 at a point C_3 . In the same way, the trajectory of \tilde{X} passing through B_2 crosses T_3 at a point D_3 . Consider C_5 an arbitrary point of the unstable separatrix of F . Let T_4 be a transversal section to X at C_5 . The section T_4 also is transversal to \tilde{X} and it crosses the unstable separatrix of \tilde{F} at D_5 . Let $C_6 \in T_3$ be a point at the right of C_4 . The trajectory of X passing through C_6 crosses T_4 at C_7 . In the same way, let $D_6 \in T_3$ be a point at the right of D_4 . The trajectory of \tilde{X} passing through D_6 crosses T_4 at D_7 . Let $C_8 \in T_4$ be a point at the right of C_5 . The trajectory of X passing through C_8 crosses Σ at A_3 . In the same way, let $D_8 \in T_4$ be a point at the right of D_5 . The trajectory of \tilde{X} passing through D_8 crosses Σ at B_3 . Now, it is enough to repeat the construction made in the previous case. The homeomorphism h sends T_1 to T_1 , the arc of trajectory $\gamma_1 = \widehat{A_1 C_3}$ to the arc of trajectory $\tilde{\gamma}_1 = \widehat{A_1 D_3}$, T_3 to T_3 , the arc of trajectory $\gamma_2 = \widehat{C_6 C_7}$ to the arc of trajectory $\tilde{\gamma}_2 = \widehat{D_6 D_7}$, T_4 to T_4 , the arc of trajectory $\gamma_3 = \widehat{C_8 A_5}$ to the arc of trajectory $\tilde{\gamma}_3 = \widehat{D_8 B_5}$, T_2 to T_2 and the arc of trajectory $\gamma_4 = \widehat{A_6 A_7}$ to the arc of trajectory $\tilde{\gamma}_4 = \widehat{A_6 B_7}$. Now we can extend continuously h to the interior of the region bounded by $T_1 \cup \gamma_1 \cup T_3 \cup \gamma_2 \cup T_4 \cup \gamma_3 \cup T_2 \cup \gamma_4$. In this way, there exists a Σ -preserving homeomorphism h that sends orbits of Z to orbits of \tilde{Z} . \square

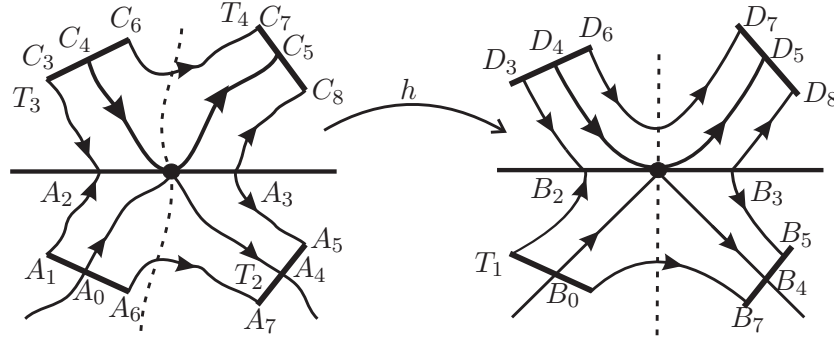


FIGURE 13. Construction of a C^0 -equivalence: Case $\tau = vis$.

6. PROOF OF THEOREM 1

Proof of Theorem 1. In Cases 1_1 , 2_1 and 3_1 we assume that Y presents the behavior Y^- . In Cases 4_1 , 5_1 and 6_1 we assume that Y presents the behavior Y^0 . In these cases canard cycles do not arise.

◊ *Cases* (1_1) $d_1 < e_1$, (2_1) $d_1 = e_1$ and (3_1) $d_1 > e_1$: The points of Σ outside the interval (d_1, e_1) (or (e_1, d_1)) belong to Σ_c . The points inside this interval, when it is not degenerate, belong to Σ_s in Case 1_1 and to Σ_2 in Case 3_1 . In both cases $H(z) > 0$ for all $z \in \Sigma_e \cup \Sigma_s$. See Figure 14.

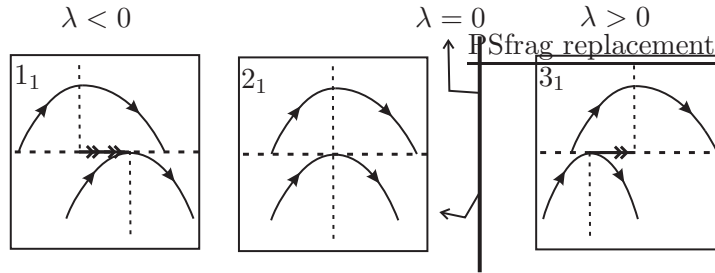


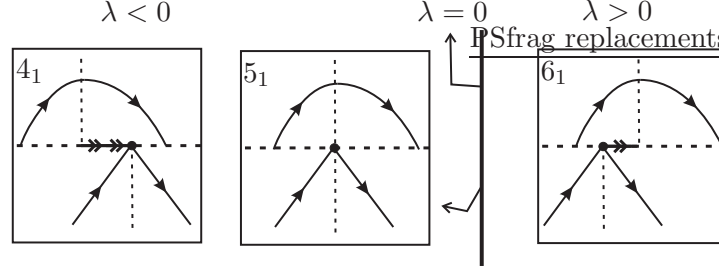
FIGURE 14. Cases 1_1 , 2_1 and 3_1 .

◊ *Cases* (4_1) $d_1 < s_1$, (5_1) $d_1 = s_1$ and (6_1) $d_1 > s_1$: The points of Σ outside the interval (d_1, s_1) (or (s_1, d_1)) belong to Σ_c . The points inside this interval, when it is not degenerate, belong to Σ_s in Case 4_1 and to Σ_2 in Case 6_1 . In both cases $H(z) > 0$ for all $z \in \Sigma_e \cup \Sigma_s$. See Figure 15.

In Cases $7_1 - 19_1$ we assume that Y presents the behavior Y^+ .

Observe that as the parameter λ increases – assuming the values L_0 , L_1 and L_2 below described – it appear orbit-arcs of X connecting the points h and i , h and j and i and j respectively.

Remembering that $\alpha = 1 - (12\beta / (-3 + 6\beta + \sqrt{9 - 12\beta^2}))$ the values of L_0 , L_1 and L_2 are:

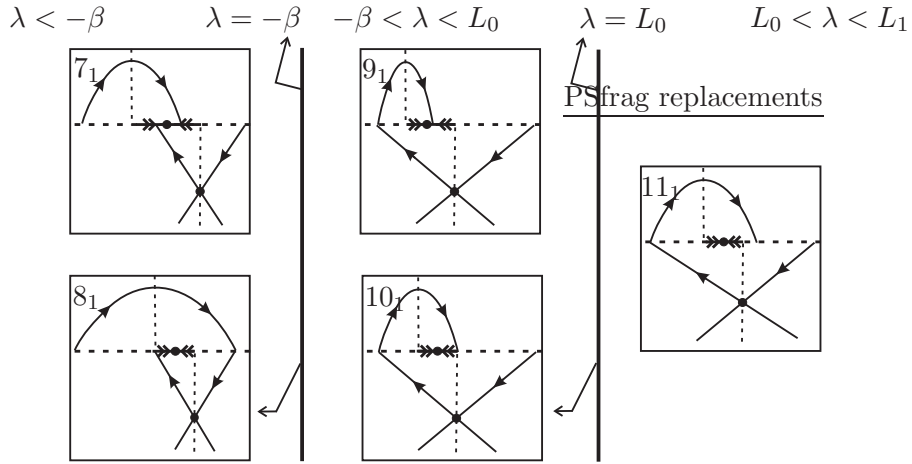
FIGURE 15. Cases 4_1 , 5_1 and 6_1 .

$$L_0 = [-9 - 6\beta + \sqrt{9 - 12\beta^2} + \sqrt{2}\sqrt{15 + \sqrt{9 - 12\beta^2} - 2\beta(-3 + 2\beta + \sqrt{9 - 12\beta^2})}]/12$$

$$L_1 = -1/2 + \sqrt{9 - 12\beta^2}/6$$

$$L_2 = [-9 + 6\beta + \sqrt{9 - 12\beta^2} + \sqrt{2}\sqrt{15 + \sqrt{9 - 12\beta^2} + 2\beta(-3 + 2\beta + \sqrt{9 - 12\beta^2})}]/12.$$

◇ *Cases* (7_1) $\lambda < -\beta$, (8_1) $\lambda = -\beta$, (9_1) $-\beta < \lambda < L_0$, (10_1) $\lambda = L_0$ and (11_1) $L_0 < \lambda < L_1$: The points of Σ outside the interval (d_1, i_1) belong to Σ_c . The points inside this interval belong to Σ_s . The direction function H assumes positive values in a neighborhood of d_1 , negative values in a neighborhood of i_1 and there exists only one value $\tilde{P} = \tilde{P}_{\lambda, \alpha, \beta}$ such that $H(\tilde{P}) = 0$. So, by (7), the Σ -attractor $P = (\tilde{P}, 0)$, nearby $(0, 0)$, is the unique pseudo equilibrium of Z . In these cases canard cycles do not arise. See Figure 16.

FIGURE 16. Cases $7_1 - 11_1$.

◇ *Case* (12_1) $\lambda = L_1$: Since $\lambda = L_1$ there is an orbit-arc γ_1^X of X connecting the points h and j . It generates a Σ -graph $\Gamma = \gamma_1^X \cup \Sigma_e \cup S \cup \Sigma_c$

of kind I. Moreover, since $\alpha = \alpha_0$, where α_0 is given by (13), there exists a non generic tangential singularity at the point $d = i$. So, the points of $\Sigma/\{d\}$ belong to Σ_c . As the Σ -fold point of X is expansive, a direct calculus shows that the *First Return Map* $\eta : (h, d) \rightarrow (h, d)$ has derivative bigger than 1. As consequence, Γ is a repeller for the trajectories inside it, $d = i$ behaves itself like an attractor (weak focus) and canard cycles do not arise. See Figure 17.

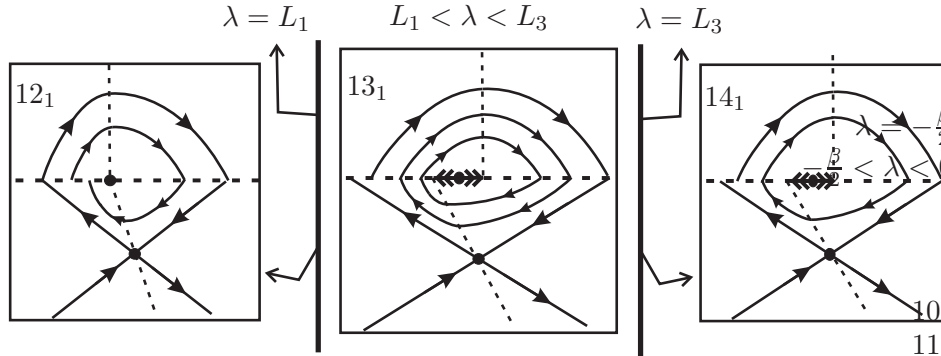


FIGURE 17. Cases 12_1 , 13_1 and 14_1 .

◇ *Case (13₁)* $L_1 < \lambda < L_3$: The meaning of L_3 will be given below in this case. The points of Σ outside the interval (i_1, d_1) belong to Σ_c and the points inside this interval belong to Σ_e . The direction function H assumes positive values in a neighborhood of d_1 , negative values in a neighborhood of i_1 and there exists a unique value $\tilde{P} = \tilde{P}_{\lambda, \alpha, \beta}$ such that $H(\tilde{P}) = 0$. So $P = (\tilde{P}, 0)$ is a Σ -repeller. When λ is a bit bigger than L_1 , the First Return Map η has two fixed points, i.e., Z has two canard cycles. One of them, called Γ_1 , is born from the bifurcation of the Σ -graph Γ of the previous case and the other one, called Γ_2 , is born from the bifurcation of the non generic tangential singularity presented in the previous case. Both of them are canard cycles of kind I. Moreover, we obtain that Γ_1 is a hyperbolic repeller canard cycle and Γ_2 is a hyperbolic attractor canard cycle. Note that, as λ increases, Γ_1 becomes smaller and Γ_2 becomes bigger. When λ assumes the limit value L_3 , one of them collides to the other. See Figure 17.

◇ *Case (14₁)* $\lambda = L_3$: The distribution of the connected components of Σ and the behavior of H are the same as Case 13_1 . Since $\lambda = L_3$, as described in the previous case, there exists a non hyperbolic canard cycle Γ of kind I which is an attractor for the trajectories inside it and is a repeller for the trajectories outside it. See Figure 17.

◇ *Cases (15₁)* $L_3 < \lambda < L_2$, (16₁) $\lambda = L_2$, (17₁) $L_2 < \lambda < \beta$, (18₁) $\lambda = \beta$ and (19₁) $\lambda > \beta$: The points of Σ outside the interval (i_1, d_1) belong to Σ_c and the points inside this interval belong to Σ_e . The direction function

H assumes positive values in a neighborhood of d_1 , negative values in a neighborhood of i_1 and there exists a unique value \tilde{P} such that $H(\tilde{P}) = 0$. So, by (7), the Σ -repeller $P = (\tilde{P}, 0)$, nearby $(0, 0)$, is the unique pseudo equilibrium of Z . In these cases canard cycles do not arise. See Figure 18.

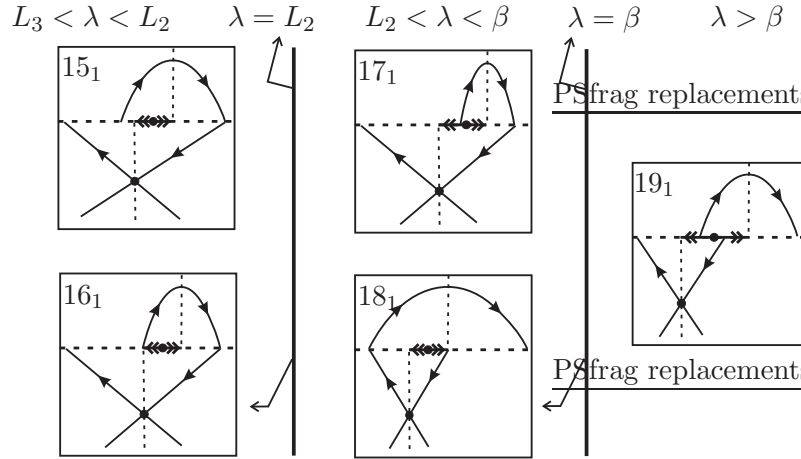


FIGURE 18. Cases $15_1 - 19_1$.

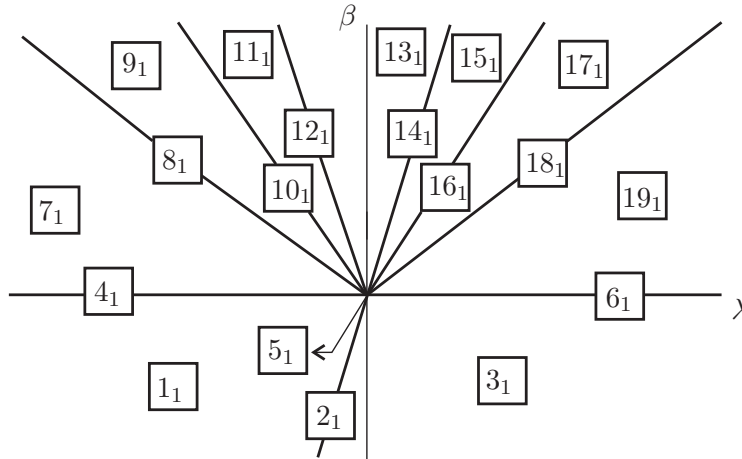


FIGURE 19. Bifurcation Diagram of Theorem 1.

The bifurcation diagram is illustrated in Figure 19. □

Remark 7. In Cases 11_1 and 15_1 the ST-bifurcations (as described in [Guardia et al.(2011)]) arise. In fact, note that the trajectory passing through

h can make more and more turns around P . This fact characterizes a global bifurcation also reached in other cases.

7. PROOF OF THEOREM 2

Proof of Theorem 2. In Cases 1_2 , 2_2 and 3_2 we assume that Y presents the behavior Y^- . In Cases 4_2 , 5_2 and 6_2 we assume that Y presents the behavior Y^0 . In Cases $7_2 - 21_2$ we assume that Y presents the behavior Y^+ .

◊ *Cases (1₂) $d_1 < e_1$, (2₂) $d_1 = e_1$, (3₂) $d_1 > e_1$, (4₂) $d_1 < s_1$, (5₂) $d_1 = s_1$ and (6₂) $d_1 > s_1$:* The analysis of these cases are done in a similar way as the cases 1_1 , 2_1 , 3_1 , 4_1 , 5_1 and 6_1 .

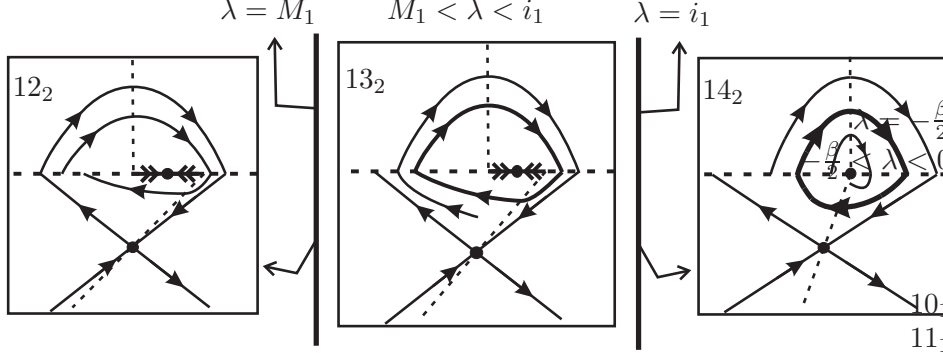
Observe that as the parameter λ increases – assuming the values M_0 , M_1 and M_2 below described – it appear orbit-arcs of X connecting the points h and i , h and j and i and j respectively. The values of M_0 , M_1 and M_2 are:

$$\begin{aligned} M_0 &= (-3 - 3\alpha(-2 + \alpha + 2(-1 + \alpha)\beta) + \\ &\quad + \sqrt{9(-1 + \alpha)^4 - 12(-1 + \alpha)^2\beta^2}) / (6(-1 + \alpha)^2), \\ M_1 &= -1/2 + \sqrt{9 - 12\beta^2}/6 \\ M_2 &= (-3 + 6\beta - 3\alpha(-2 + \alpha + 2\beta) + \\ &\quad + \sqrt{9(-1 + \alpha)^4 - 12(-1 + \alpha)^2\alpha^2\beta^2}) / (6(-1 + \alpha)^2). \end{aligned}$$

◊ *Cases (7₂) $\lambda < -\beta$, (8₂) $\lambda = -\beta$, (9₂) $-\beta < \lambda < M_0$, (10₂) $\lambda = M_0$ and (11₂) $M_0 < \lambda < M_1$:* Analogous to Cases $7_1 - 11_1$ changing L_0 by M_0 and L_1 by M_1 .

◊ *Case (12₂) $\lambda = M_1$:* The points of Σ outside the interval (d_1, i_1) belong to Σ_c and the points inside this interval belong to Σ_s . The direction function H assumes positive values in a neighborhood of d_1 , negative values in a neighborhood of i_1 (see Remark 6) and there exists a unique value $\tilde{P} = \tilde{P}_{\lambda, \alpha, \beta}$ such that $H(\tilde{P}) = 0$. So $P = (\tilde{P}, 0)$ is a Σ -attractor. Since $\lambda = M_1$, there is an orbit-arc γ_1^X of X connecting the points h and j . It generates a Σ -graph $\Gamma = \gamma_1^X \cup \Sigma_e \cup S \cup \Sigma_c$ of kind I. Since $\alpha > \alpha_0$, where α_0 is given by (13), it is straightforward to show that the *First Return Map* defined in the interval $(h_1, d_1) \subset \Sigma$ do not have fixed points. By consequence, Γ is a repeller for the trajectories inside it and canard cycles do not arise. See Figure 20.

◊ *Case (13₂) $M_1 < \lambda < i_1$:* The distribution of the connected components of Σ and the behavior of H are the same as Case 12₂. Since $M_1 < \lambda < i_1$, there is an orbit-arc γ_1^X of X connecting j to a point $k = (k_1, 0) \in \Sigma$, where $k_1 \in (h_1, d_1)$, for negative time. Also there is an orbit-arc γ_1^Y of Y connecting k to a point $l = (l_1, 0) \in \Sigma$, where $l_1 \in (i_1, j_1)$, for negative time. Repeating this argument, we can find an increasing sequence $(k_i)_{i \in \mathbb{N}}$. We can prove that there is an interval $I \subset (k, d)$ such that $\eta' = (\varphi_Y \circ \varphi_X)' < 1$ on I . As P is a Σ -attractor, there is an interval $J \subset (k, d)$ such that $\eta' > 1$ on J . Moreover, we can prove that η has a unique fixed point $Q \in (k, d)$. As consequence, there passes through Q a repeller canard cycle Γ of kind I. See Figure 20. This canard cycle is born from the bifurcation of the Σ -graph present in Case 12₂. The expression of η is too large, so the

FIGURE 20. Cases 12_2 , 13_2 and 14_2 .

general case will be omitted. For the particular case when $\alpha = -1$, $\beta = 1/2$ and $\lambda = -1/2 + 11\sqrt{6}/60$, the map η is given by

$$\eta(x) = \frac{3}{4} + \frac{3}{2} \left(-\frac{1}{2} + \frac{11}{10\sqrt{6}} \right) + \frac{x}{2} + \frac{-\frac{1}{4}\sqrt{3} \sqrt{\left(1 - 2\left(-\frac{1}{2} + \frac{11}{10\sqrt{6}}\right) - 2x\right) \left(3 + 2\left(-\frac{1}{2} + \frac{11}{10\sqrt{6}}\right) + 2x\right)}}{1}$$

A straightforward calculation shows that the unique fixed point of this particular η occurs when $x = -\sqrt{29/2}/10$.

◊ *Case (14₂) $\lambda = i_1$* : Every point of Σ belongs to Σ_c except the point $d = i$. The canard cycle presented in the previous case is persistent for this case (remember that this canard cycle is born from the bifurcation of the Σ -graph of Case 12_2 . So, its radius does not tend to zero when λ tends to i_1). So the non generic tangential singularity $d = i$ behaves itself like a weak attractor focus. See Figure 20.

◊ *Cases (15₂) $i_1 < \lambda < M_3$ and (16₂) $\lambda = M_3$* : Analogous to Cases $13_1 - 14_1$ replacing L_1 by i_1 and L_3 by M_3 , where M_3 is the limit value for which Γ_1 collides with Γ_2 .

◊ *Cases (17₂) $M_3 < \lambda < M_2$, (18₂) $\lambda = M_2$, (19₂) $M_2 < \lambda < \beta$, (20₂) $\lambda = \beta$ and (21₂) $\lambda > \beta$* : Analogous to Cases $15_1 - 19_1$ replacing L_2 by M_2 and L_3 by M_3 .

The bifurcation diagram is illustrated in Figure 21. □

8. PROOF OF THEOREM 3

Proof of Theorem 3. In Cases 1_3 , 2_3 and 3_3 we assume that Y presents the behavior Y^- . In Cases 4_3 , 5_3 and 6_3 we assume that Y presents the behavior Y^0 . In Cases $7_3 - 21_3$ we assume that Y presents the behavior Y^+ .

◊ *Cases (1₃) $d_1 < e_1$, (2₃) $d_1 = e_1$, (3₃) $d_1 > e_1$, (4₃) $d_1 < s_1$, (5₃) $d_1 = s_1$ and (6₃) $d_1 > s_1$* : Analogous to Cases 1_1 , 2_1 , 3_1 , 4_1 , 5_1 and 6_1 .

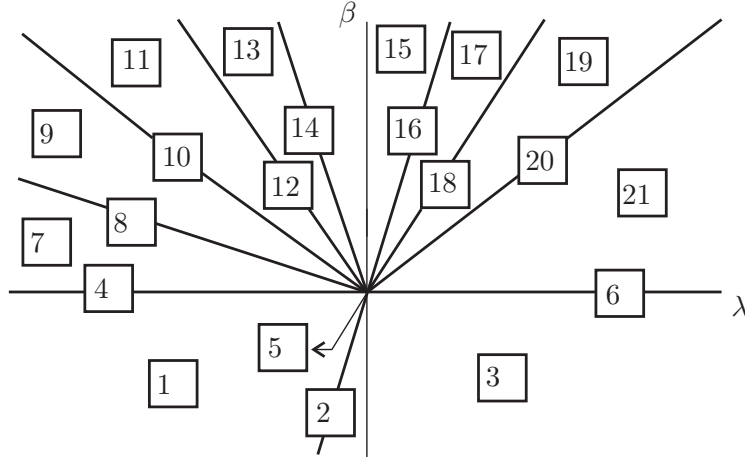


FIGURE 21. Bifurcation Diagram of Theorems 2 and 3.

In what follows we consider M_0 , M_1 , M_2 and M_3 as in the previous theorem.

◊ *Cases (7₃)* $\lambda < -\beta$, *(8₃)* $\lambda = -\beta$, *(9₃)* $-\beta < \lambda < M_0$, *(10₃)* $\lambda = M_0$ and *(11₃)* $M_0 < \lambda < i_1$: Analogous to Cases 7₂ – 11₂ changing M_1 by i_1 .

◊ *Case (12₃)* $\lambda = i_1$: Every point of $\Sigma/\{d\}$ belongs to Σ_c . In a similar way as Case 13₂, we can construct sequences $(k_i)_{i \in \mathbb{N}}$ and $(l_i)_{i \in \mathbb{N}}$. Since $d = i$ we have that $k_i \rightarrow d$ and $l_i \rightarrow d$. So d is a non generic tangential singularity that behaves itself like an attractor. See Figure 22.

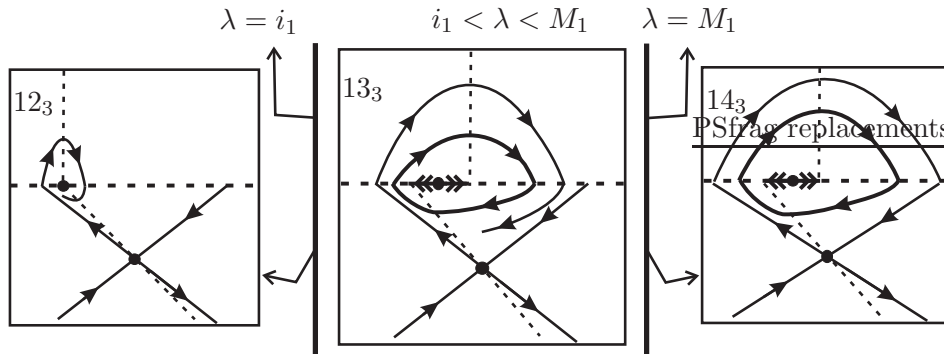


FIGURE 22. Cases 12₃, 13₃ and 14₃.

◊ *Case (13₃)* $i_1 < \lambda < M_1$: Analogous to Case 13₂ except that there is a change of stability on $P = (\tilde{P}, 0)$, which is a Σ -repeller, and on Γ , which is an attractor canard cycle of kind I. This canard cycle is born from the

bifurcation of the non-generic tangential singularity of Case 12₃. See Figure 22.

◇ *Case (14₃)* $\lambda = M_1$: Analogous to Case 12₂ except that occurs a change of stability on $P = (\tilde{P}, 0)$, which is a Σ -repeller. This fact generates a bifurcation like Hopf near P and there appears a hyperbolic attractor canard cycle Γ_1 , of kind I, between P and the Σ -graph Γ_2 . See Figure 22.

◇ *Cases (15₃)* $M_1 < \lambda < M_3$ and (16₃) $\lambda = M_3$: Analogous to Cases 15₂ – 16₂, replacing i_1 by M_1 .

◇ *Cases (17₃)* $M_3 < \lambda < M_2$, (18₃) $\lambda = M_2$, (19₃) $M_2 < \lambda < \beta$, (20₃) $\lambda = \beta$ and (21₂) $\lambda > \beta$: Analogous to Cases 17₂ – 21₂.

The bifurcation diagram is illustrated in Figure 21. □

9. PROOF OF THEOREM 4

Proof of Theorem 4. Since X has a unique Σ -fold point which is visible we conclude that canard cycles do not arise.

In Cases 1₄, 2₄ and 3₄ we assume that Y presents the behavior Y^- . In Cases 4₄, 5₄ and 6₄ we assume that Y presents the behavior Y^0 . In these cases, when it is well defined, the direction function H assumes positive values.

◇ *Case (1₄)* $d_1 < e_1$: The points of Σ inside the interval (d_1, e_1) belong to Σ_c . The points on the left of d_1 belong to Σ_s and the points on the right of e_1 belong to Σ_e . See Figure 23.

◇ *Case (2₄)* $d_1 = e_1$: Here $\Sigma_c = \emptyset$. The vector fields X and Y are linearly dependent on $d_1 = e_1$ which is a tangential singularity. Moreover, it is an attractor for the trajectories of Z crossing Σ_s and a repeller for the trajectories of Z crossing Σ_e . See Figure 23.

◇ *Case (3₄)* $d_1 > e_1$: The points of Σ inside the interval (e_1, d_1) belong to Σ_c . The points on the left of e_1 belong to Σ_s and the points on the right of d_1 belong to Σ_e . See Figure 23.

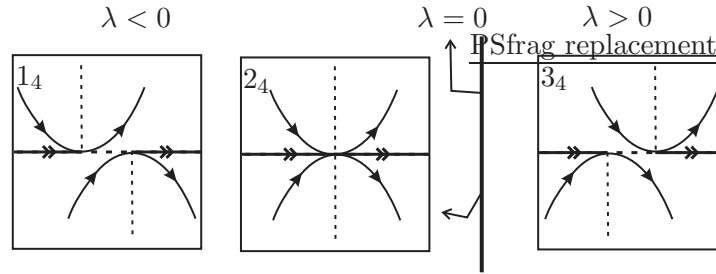


FIGURE 23. Cases 1₄, 2₄ and 3₄.

◇ *Case (4₄)* $d_1 < s_1$: The points of Σ inside the interval (d_1, s_1) belong to Σ_c . The points on the left of d_1 belong to Σ_s and the points on the right of s_1 belong to Σ_e . See Figure 24.

◊ *Case (5₄)* $d_1 = s_1$: Here $\Sigma_c = \emptyset$ and S is an attractor for the trajectories of Z crossing Σ_s and it is a repeller for the trajectories of Z crossing Σ_e . See Figure 24.

◊ *Case (6₄)* $d_1 > s_1$: The points of Σ inside the interval (d_1, s_1) belong to Σ_c . The points on the left of s_1 belong to Σ_s and the points on the right of d_1 belong to Σ_e . See Figure 24.

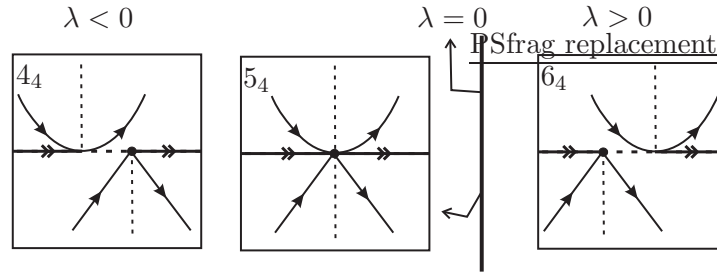


FIGURE 24. Cases 4₄, 5₄ and 6₄.

In Cases 7₄ – 13₄ we assume that Y presents the behavior Y^+ .

◊ *Cases (7₄)* $d_1 < h_1$, (8₄) $d_1 = h_1$ and (9₄) $h_1 < d_1 < i_1$: The points of Σ inside the interval (d_1, i_1) belong to Σ_c . The points on the left of d_1 belong to Σ_s and the points on the right of i_1 belong to Σ_e . The direction function H assumes positive values on Σ_s and negative values in a neighborhood of i_1 . Moreover, $H(\beta\lambda/(-1+\beta)) = 0$ and the Σ -repeller $P = (\beta\lambda/(-1+\beta), 0)$ is the unique pseudo equilibrium. See Figure 25.

◊ *Case (10₄)* $d_1 = i_1$: Here $\Sigma_c = \emptyset$. The vector fields X and Y are linearly dependent on the tangential singularity $d_1 = i_1$. A straightforward calculation shows that $H(z) = (1 - \beta)/2 \neq 0$ for all $z \in \Sigma/\{d\}$. So $d_1 = i_1$ is an attractor for the trajectories of Z crossing Σ_s and a repeller for the trajectories of Z crossing Σ_e . Moreover, $\Delta = \{d\} \cup \overline{dj} \cup \Sigma_e \cup \{S\} \cup \Sigma_c \cup \overline{hd}$ is a Σ -graph of kind III in such a way that each Q in its interior belongs to another Σ -graph of kind III passing through d . See Figure 25.

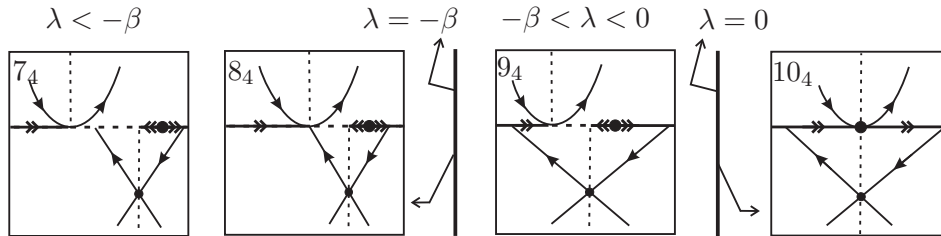


FIGURE 25. Cases 7₄ – 10₄.

◊ *Cases (11₄)* $i_1 < d_1 < j_1$, *(12₄)* $d_1 = j_1$ and *(13₄)* $j_1 < d_1$: The points of Σ inside the interval (i_1, d_1) belong to Σ_c . The points on the left of i_1 belong to Σ_s and the points on the right of d_1 belong to Σ_e . The direction function H assumes positive values on Σ_e and negative values in a neighborhood of i_1 . Moreover, $H(\beta\lambda/(-1 + \beta)) = 0$ and the Σ -attractor $P = (\beta\lambda/(-1 + \beta), 0)$ is the unique pseudo equilibrium. See Figure 26.

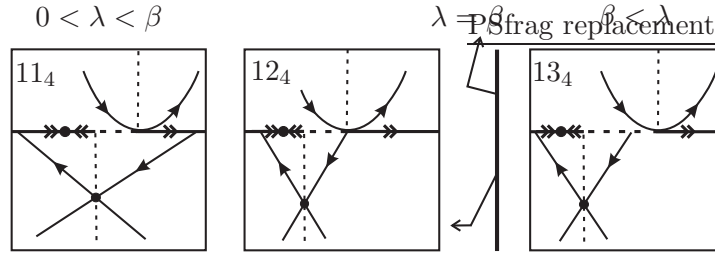


FIGURE 26. Cases 11₄ – 13₄.

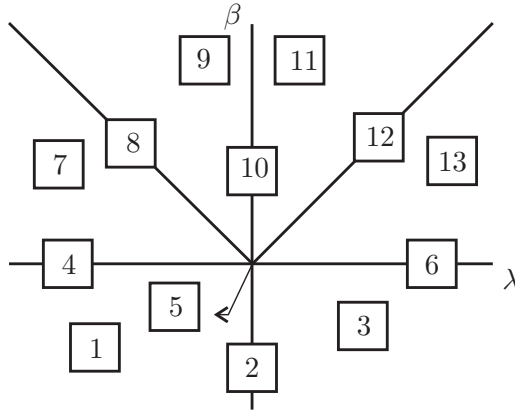


FIGURE 27. Bifurcation Diagram of Theorems 4, 5 and 6.

The bifurcation diagram is illustrated in Figure 27. □

10. PROOF OF THEOREM 5

Proof of Theorem 5. The direction function H has a root $Q = (q, 0)$ where

$$(14) \quad q = \frac{1}{2(\alpha + 1)} \left((-1 + \alpha)(1 - \beta) - \lambda(1 + \alpha) + \sqrt{((-1 + \alpha)(1 - \beta) - \lambda(1 + \alpha))^2 + 4\beta(1 + \alpha)(1 + \alpha + \lambda(-1 + \alpha))} \right).$$

Moreover, H assumes positive values on the right of Q and negative values on the left of Q . Note that when $\alpha \rightarrow -1$ so $Q \rightarrow -\infty$ under the line $\{y = 0\}$ and it occurs the configurations showed in Theorem 4.

In Cases 1_5 , 2_5 and 3_5 we assume that Y presents the behavior Y^- . In Cases 4_5 , 5_5 and 6_5 we assume that Y presents the behavior Y^0 . In Cases $7_5 - 13_5$ we assume that Y presents the behavior Y^+ .

◇ *Cases* (1_5) $d_1 < e_1$, (2_5) $d_1 = e_1$, (3_5) $d_1 > e_1$, (4_5) $d_1 < s_1$, (5_5) $d_1 = s_1$ and (6_5) $d_1 > s_1$: Analogous to Cases 1_4 , 2_4 , 3_4 , 4_4 , 5_4 and 6_4 respectively, except that here it appears the Σ -saddle Q on the left of d and e or S . See Figure 28.

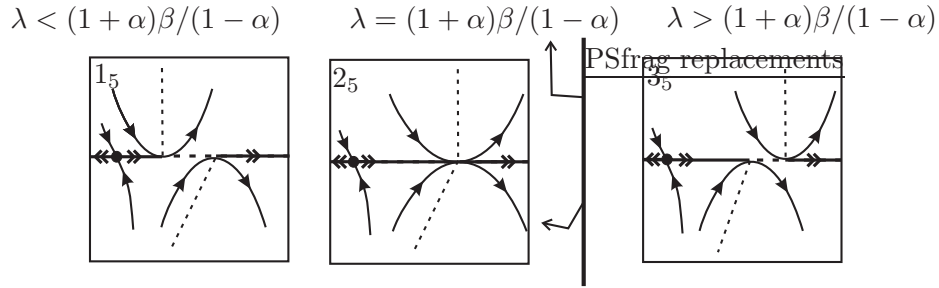


FIGURE 28. Cases 1_5 , 2_5 and 3_5 .

◇ *Cases* (7_5) $d_1 < h_1$, (8_5) $d_1 = h_1$, (9_5) $h_1 < d_1 < i_1$: Analogous to Cases $7_4 - 9_4$, except that here the Σ -saddle Q appears on the left of d_1 and i_1 . So $P = (p, 0)$ where

$$(15) \quad p = \frac{1}{2(\alpha + 1)} \left((-1 + \alpha)(1 - \beta) - \lambda(1 + \alpha) + \sqrt{((-1 + \alpha)(1 - \beta) - \lambda(1 + \alpha))^2 + 4\beta(1 + \alpha)(1 + \alpha + \lambda(-1 + \alpha))} \right).$$

◇ *Case* (10_5) $d_1 = i_1$: Analogous to Case 10_4 , except that here appear the Σ -saddle Q on the left of $d_1 = i_1$.

◇ *Cases* (11_5) $i_1 < d_1 < j_1$, (12_5) $d_1 = j_1$ and (13_5) $j_1 < d_1$: Analogous to Cases $11_4 - 13_4$, except that here the Σ -saddle Q appears on the left of d_1 and i_1 .

The bifurcation diagram is illustrated in Figure 27. □

11. PROOF OF THEOREM 6

Proof of Theorem 6. The direction function H has a root $Q = (q, 0)$ where q is given by (14). Moreover, H assumes positive values on the left of Q and negative values on the right of Q . Note that when $\alpha \rightarrow -1$ so $Q \rightarrow \infty$ under the line $\{y = 0\}$ and the configurations shown in Theorem 4 occur.

In Cases 1_6 , 2_6 and 3_6 we assume that Y presents the behavior Y^- . In Cases 4_6 , 5_6 and 6_6 we assume that Y presents the behavior Y^0 . In Cases $7_6 - 13_6$ we assume that Y presents the behavior Y^+ .

◊ *Cases* (1_6) $d_1 < e_1$, (2_6) $d_1 = e_1$, (3_6) $d_1 > e_1$, (4_6) $d_1 < s_1$, (5_6) $d_1 = s_1$ and (6_6) $d_1 > s_1$, (7_6) $d_1 < h_1$, (8_6) $d_1 = h_1$, (9_6) $h_1 < d_1 < i_1$, (10_6) $d_1 = i_1$, (11_6) $i_1 < d_1 < j_1$, (12_6) $d_1 = j_1$ and (13_6) $j_1 < d_1$: Analogous to Cases 1_5 , 2_5 , 3_5 , 4_5 , 5_5 , 6_5 , 7_5 , 8_5 , 9_5 , 10_5 , 11_5 , 12_5 and 13_5 respectively, except that here the Σ -saddle Q takes place on the right of d_1 , e_1 , s_1 and i_1 when these points appear.

The bifurcation diagram is illustrated in Figure 27. \square

Acknowledgments. The first and the third authors are partially supported by a FAPESP-BRAZIL grant 2007/06896-5. The second author was partially supported by FAPESP-BRAZIL grants 2007/08707-5, 2010/18190-2 and 2012/00481-6.

REFERENCES

- [Andronov & Pontryagin(1937)] Andronov, A. & Pontryagin, S. [1937] “Structurally stable systems,” *Dokl. Akad. Nauk SSSR*, **14**, 247–250.
- [di Bernardo *et al.*(2008)] di Bernardo, M., Budd, C.J., Champneys, A.R. & Kowalczyk, P. [2008] “Piecewise-smooth Dynamical Systems – Theory and Applications,” (Springer-Verlag).
- [di Bernardo *et al.*(2008)] di Bernardo, M., Budd, C.J., Champneys, A.R., Kowalczyk, P., Nordmark, A.B., Tost, G.O. & Piiroinen, P.T. [2008] “Bifurcations in nonsmooth dynamical systems,” *SIAM Rev.*, **50**, 629–701.
- [di Bernardo *et al.*(2006)] di Bernardo, M., Champneys, A.R., Hogan, S.J., Homer, M., Kowalczyk, P., Kuznetsov, Yu.A., Nordmark, A.B., Tost, G.O. & Piiroinen, P.T. [2006] “Two-parameter discontinuity-induced bifurcations of limit cycles: classification and open problems,” *International Journal of Bifurcation and Chaos*, **16**, 601–629.
- [Buzzi *et al.*(2010)] Buzzi, C.A., de Carvalho, T. & da Silva, P.R. [2010] “Closed poly-trajectories and Poincaré Index of non-smooth vector fields on the plane,” *preprint*. Posted in arXiv:1002.4169v1 [math.DS].
- [Coll *et al.*(2000)] Coll, B., Gasull, A. & Prohens, R. [2000] “Center-focus and isochronous center problems for discontinuous differential equations,” *Discrete and Continuous Dynamical Systems*, **6**, 609–624.
- [Dumortier (1978)] Dumortier, F. [1978] *Singularities of Vector Fields*, Monografias de Matemática 32 (IMPA, Brazil).
- [Dumotier & Roussarie(1996)] Dumortier, F. & Roussarie, R. [1996] “Canard cycles and center manifolds,” *Memoirs Amer. Mat. Soc.*, **121**.
- [Filippov(1988)] Filippov, A.F. [1988] *Differential equations with discontinuous righthand sides*, Mathematics and its Applications (Soviet Series) (Kluwer Academic Publishers-Dordrecht, Russia).
- [Glendinning(2004)] Glendinning, P. [2004] “Non-smooth pitchfork bifurcations,” *Discrete and Continuous Dynamical Systems Ser. B*, **4**, 457–464.
- [Guardia *et al.*(2011)] Guardia, M., Seara, T.M. & Teixeira, M.A. [2011] “Generic bifurcations of low codimension of planar Filippov Systems,” *Journal of Differential Equations*, **250**, 1967–2023.
- [Kozlova(1984)] Kozlova, V.S. [1984] “Roughness of a discontinuous system,” *Vestnik Moskovskogo Universiteta, Matematika*, **5**, 16–20.

- [Kuznetsov *et al.*(2003)] Kuznetsov, YU.A., Rinaldi, S. & Gragnani, A. [2003] “One-parameter bifurcations in planar Filippov systems,” *International Journal of Bifurcation and Chaos*, **13**, 2157–2188.
- [Roy & Roy(2008)] Roy, I. & Roy, A.R. [2008] “Border collision bifurcations in three-dimensional piecewise smooth systems,” *International Journal of Bifurcation and Chaos*, **18** (2), 577–586.
- [Sotomayor(1974)] Sotomayor, J. [1974] “Generic one-parameter families of vector fields on two-dimensional manifolds,” *Inst. Hautes tudes Sci. Publ. Math.*, **43**, 5–46.
- [Teixeira(1977)] Teixeira, M.A. [1977] “Generic bifurcation in manifolds with boundary,” *Journal of Differential Equations*, **25**, 65–88.
- [Teixeira(1979)] Teixeira, M.A. [1979] “Generic bifurcation of certain singularities,” *Bollettino della Unione Matematica Italiana* (5), **16-B**, 238–254.
- [Teixeira(1991)] Teixeira, M.A. [1991] “Generic singularities of discontinuous vector fields,” *An. Ac. Bras. Cienc.*, **53**, 257–260.
- [Teixeira(2008)] Teixeira, M.A. [2008] *Perturbation theory for non-smooth systems*, Meyers: Encyclopedia of Complexity and Systems Science 152.
- [Vishik(1972)] Vishik, S.M. [1972] “Vector fields near the boundary of a manifold,” *Vestnik Moskovskogo Universiteta, Matematika*, **27**, 21–28.

¹ IBILCE–UNESP, CEP 15054–000, S. J. RIO PRETO, SÃO PAULO, BRAZIL

² FC–UNESP, BAURU, SÃO PAULO, BRAZIL

³ IMECC–UNICAMP, CEP 13081–970, CAMPINAS, SÃO PAULO, BRAZIL

E-mail address: `buzzi@ibilce.unesp.br`

E-mail address: `tcarvalho@fc.unesp.br`

E-mail address: `teixeira@ime.unicamp.br`

